

# Spectroscopy of Ion Lasers

WILLIAM B. BRIDGES, MEMBER, IEEE, AND ARTHUR N. CHESTER

**Abstract**—A brief review of the history of laser oscillation in gaseous ions is given, including a tabulation of wavelengths, classifications, and references for the 230 reported ion laser transitions. Selection rules and excitation mechanisms yielding oscillation are discussed.

## HISTORY

OVER 200 new wavelengths were added to the growing list of laser lines in 1964 by virtue of laser action in the ions of 11 gases. In this paper we will attempt to review this brief history of the ion laser, list the laser transitions observed to date, including a few of their salient characteristics, and attempt to summarize what is known about the conditions necessary to obtain laser action in ions. Such a task is difficult at the fast pace of today's research, but we have attempted to make this review accurate and up-to-the-minute.

Laser action in gaseous ions was first observed by Bell [1], who obtained oscillation on green, orange, and infrared transitions in singly ionized mercury (Hg II). It is interesting that this first discovery demonstrated improvement in three technologically important characteristics: 1) high power (several watts peak), 2) high gain (more than 20 per cent per meter), and 3) short wavelength visible operation (green).

Bell's discovery was followed by the independent and almost simultaneous discovery of several powerful blue and green lines in Ar II by Bridges [2], Convert, et al. [3], [4], and Bennett, et al. [5]. Optical gains of several decibels per meter and long-pulse (i.e., microseconds or longer) power outputs of several watts were reported for a few of these lines [5]. Shortly thereafter, oscillation spanning the entire visible spectrum was obtained in Kr II and Xe II by Bridges [6]. Again, high gain and high power were obtained. Meanwhile, the spectroscopy of mercury lasers had been extended into the infrared by Bloom, Bell, and Lopez [7] and into the blue with an Hg III line observed by Gerritsen and Goedertier [8].

All of the observations just cited were made with pulsed discharges. Except for the Hg II lines, which were obtained only in the discharge afterglow [9], laser oscillation was observed to begin and end promptly with the current pulse. Quasi-cw operation, i.e., with pulse durations longer than the time constants of any reasonable atomic process, was reported in Ar II by Bennett, et al. [5], who obtained output powers of watts for about a millisecond. Continuous operation (i.e., minutes to hours) at the 0.1-watt level was obtained about the same time

by Gordon, Labuda, and Bridges [10] on most of the stronger Ar II, Kr II, and Xe II lines. Gas motion and heating effects with time constants of the order of seconds [10], [11] were found to be important in true continuous operation, so that results obtained under quasi-cw conditions do not extend directly (to say nothing of the thermal and structural complications caused by the higher average power inputs in continuous operation).

McFarlane [12] added nitrogen, oxygen, and carbon to the list of ion laser materials, including visible and ultraviolet lines of singly, doubly, and triply ionized atoms. Bridges and Chester had also seen and identified a number of the oxygen lines by this time [13].

Oscillation in singly ionized iodine was observed in an iodine-helium discharge by Fowles and Jensen [14], [15]. The laser output was observed only in the afterglow, similar to the Hg II lines, implying that collisions with helium atoms rather than electrons is the excitation mechanism. Several chlorine ion lines were reported by McFarlane [16], as well as three ultraviolet Ar III lines.

Ion lines excited by collisions of the second kind were also observed in the noble gases by Laures, Dana, and Frapard [17]–[19]. They obtained afterglow oscillation on Kr II lines in a helium-krypton discharge and on Xe II lines in a neon-xenon discharge.

A survey of the noble gases was made by Bridges and Chester [13], who obtained oscillation on ultraviolet lines in neon and other noble gases, as well as many new visible transitions. A similar survey was made in the ultraviolet by Cheo and Cooper [20], who have also observed new transitions in nitrogen, oxygen, and the noble gases.

Further spectroscopic work by other investigators has added new transitions to the list. Several new lines in the noble gases were discovered in the near infrared by Sinclair [21] and in the ultraviolet by Dana, Laures, and Rocherolles [22]. Additional lines were seen in the near infrared by Horrigan, Koozekanani, and Paananen [23], and in the visible by Bloom and Bell [9] and Birnbaum and Stocker [24]. New iodine lines were reported by Jensen and Fowles [25], [26] and additional nitrogen lines by McFarlane [27]. A number of lines have been reported by Heard, Makhov, and Peterson [28]–[31], but their measurement of wavelength was not sufficiently accurate to establish them as lines not previously observed by others [32].

Lifetimes of some of the Ar II laser transitions have been measured by Bennett, et al. [33]. Gordon, Labuda, and Miller [34] have made extensive measurements of line intensities and gains of these and other lines in order to determine the relevant internal population and depopulation processes. Their analysis will appear shortly [35].

## TABLES

## Table II: Neon

A listing of all the ion laser wavelengths reported to date appears in Tables II to XII, with the explanation of the abbreviations appearing in Table I. The calculated wavelengths were computed from energy levels tabulated in *Atomic Energy Levels* [36], using the refractive index corrections given in *Table of Wavenumbers* [37], unless otherwise indicated. Some of the Ar II lines are more accurately given by the recent wavelength measurements of Minnhagen [38], and for these lines we have entered his values (rounded to the nearest 0.01 Angstrom). The recent spectral analysis of I II by Martin and Corliss [39] has been used for the iodine wavelengths.

When wavelengths could not be assigned to known energy levels, a brief search of the spectroscopic literature was made to determine whether the line in question had been observed in spontaneous emission. In most cases, the lines were observed many years ago but remained unclassified. Most notably, strong and characteristic unidentified laser lines in the xenon had been observed by Humphreys [40] as strong lines in spontaneous emission but were not reported since no identification was made. Although we cannot properly assess the wavelength accuracy of the older references [41]–[44], we have listed their values in the “calculated wavelength” column when so indicated. The main value of such entries is to offer some spectroscopic confirmation for the existence of the observed laser line in the gas under which it is listed; since most workers have used different gases in the same discharge tube, either simultaneously or sequentially, there is often a question as to the source of an unidentified line.

The lines that were observed only in the discharge afterglow are believed to arise from upper levels that are populated by collisions in gas mixtures in a manner analogous to the helium-neon laser. In all cases, lines observed in the afterglow were obtained only in gas mixtures and were not obtainable during the current pulse, with only two special exceptions. W. E. Bell (private communication) reports that the line Hg II 6150 oscillates during the current pulse in a hollow cathode discharge; the other line, Xe II 5727, is discussed in the appropriate section of this paper.

A more detailed discussion of each table follows. All wavelengths given in the tables and in the text are in Angstroms, the “Å” being omitted for brevity. We have chosen to specify the core configuration explicitly in the designation of energy levels listed in the *classification* column, rather than use the “prime,” “double prime,” etc., notation [36]. Although the notation with primes is unambiguous for the noble gases, confusion is possible with oxygen and nitrogen because cores with both parities occur in each ionization state. In gases other than oxygen and nitrogen, where no confusion would occur, the core is omitted for the “unprimed” levels and specified for the others.

The line 2473 was assigned to the transition  $a^3D_3 \rightarrow ({}^2D) 3p^3P_2$  by de Bruin [41] but there is some dispute about this classification, and the upper level he gives is not listed in *Atomic Energy Levels*. The assignment Ne III is made by Cheo and Cooper [20] from work by Minnhagen (private communication). The lines 2678 and 2679 were both observed to oscillate by Cheo and Cooper [20]; these two lines were not resolved in the previous work of Bridges and Chester [13]. The possible assignment of 2867 to Ne IV was made on the basis of observed time behavior and current dependence [13]. To our knowledge, the line 3331 has not been seen in spontaneous emission; therefore its identification as an intercombination line remains somewhat questionable.

The only two neon lines that are not of the form  $p \rightarrow s$  are 3329 and 3393, which are both  $3d \rightarrow 3p$ . However, the lower level of 3329 is the upper level of the strong spontaneous line at 3334.87 (de Bruin [45]); likewise, the strong spontaneous lines 3713.09 and 3230.16 originate from the lower level of 3393.20 [45]. If the assignments for these two lines are correct, it is evidently possible to obtain the necessary inversion on these two transitions even though they do not obey the  $p \rightarrow d$  or  $p \rightarrow s$  “rules” followed by most of the pure-gas ion laser lines.

Attempts by Bridges and Chester to produce continuous oscillation on the lines 3323.77, 3378.30, or 3392.86 in a 20-cm tube have proved unsuccessful to date; high-reflectance dielectric mirrors [13] and discharge inputs up to 7 kW were used [46].

## Table III: Argon

Minnhagen and Stigmark [47] assign the line 2754 to Ar III, although they have not published their measured value; the “calculated wavelength” reported is the older value given by Rosenthal [42]. The more accurate measurement of Cheo and Cooper on the line 3002.64 precludes the  $f \rightarrow d$  assignment originally given by Bridges and Chester [13] and repeated by Dana, Laures, and Rocherolles [22]. Again, the “calculated” value is from Rosenthal and is not necessarily better than Cheo and Cooper’s measured value. Only one “backward” line ( $d \rightarrow p$ ), 3576.61, is observed, and this line terminates on the strong (laser and spontaneous) line 5145. The line 3638 has been classified by McFarlane [16] by analogy with the isoelectronic transitions in Cl II; the existence of a yet unidentified argon line nearby (3705) makes identification on this basis somewhat questionable, however. The wavelength measurement of the line 4147 differs from the calculated value by an amount outside the estimated error; nevertheless, this remains a likely identification since the line 5502 has the same lower level. The line 4183 is identified as Ar III, since it is not listed in Minnhagen’s extensive monograph on Ar II [38], but it was much stronger and occurred at much lower currents than

the two "choice" ( $\Delta J = \Delta L = +1$ )<sup>1</sup> Ar IV lines, 2913 and 2926.

The several strong blue and green lines listed in the first announcement of laser action in Ar II [2] have been studied by many workers. The intensity of the effort expended on these few transitions makes any listing of gain, output power, etc., subject to immediate obsolescence. We report here what is known at the present time. Ten visible lines [10] and the 1.09-micron line [46] have been obtained in cw operation.

Reported output powers have been revised upward on an almost monthly basis. The original report of cw operation [10] quoted 80-mW total output (each end) in the six strongest lines using a 20-cm discharge; the authors have now observed 2W in a single line (4880) in a 50-cm discharge. Gordon and Labuda report 4-W output at 0.2-per cent efficiency in a 60-cm discharge [34]. Paananen reports 7-W output in a 90-cm discharge [49]. These last three results were obtained with a longitudinal magnetic field to compress the plasma, as originally suggested by Gordon and Labuda [34]. Pulsed power output runs even higher; Bennett, et al. [5] report several hundred watts output with very short excitation pulses (20 ns) in a 3-m-long tube. The authors have seen peak power over 40W and average power of 0.1W with 20  $\mu$ s pulses in a 1-m tube [46].

Gain measurements vary with the particular experimental arrangement. Bennett reports pulsed gains for seven of the strongest lines: 4579, 0.6 dB/m; 4658, 0.7 dB/m; 4765, > 3.7 dB/m; 4880, 3 dB/m; 4965, 2.8 dB/m; 5017, 1.0 dB/m; and 5145, 2.1 dB/m. The authors have measured pulsed gains of 7 dB/m at 4765 and 13 dB/m at 4880 [46]; Gordon and Labuda report a cw gain of over 20 dB/m at 4880 [34].

Three weaker lines at 4609, 4889, and 5141 were observed by the authors [13] in a 3-mm diameter, 2-m-long discharge in the same wavelength range covered by their earlier work. Birnbaum and Stocker [24], using higher reflectivity mirrors, were able to obtain these weak lines in a 2-mm by 30-cm tube; they also observed a new line, 4992.55. The assignment of this line to Ar III is made on the basis of the similarity in threshold to Ar III 5502 (which was obtained simultaneously in their tube) and the fact that the spectrum Ar II has been extremely well covered by Minnhagen [38].

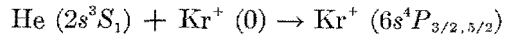
Although the assignment given for the line 8772 lies outside the estimated measurement error, Sinclair agrees [50] that the assignment given is correct. Both upper and lower level are shared with other laser lines, and the relative time behavior should confirm or deny the assignment. (Relative time behavior was used as an additional check by the authors in the case of the line 5017.16 [2], [46]; the incorrect assignment of this line to the transition at 5017.63 [48] was reported by Convert, et al. [4].)

<sup>1</sup> As in [13],  $\Delta$  means (upper)-(lower).

Table IV: Krypton

We have tentatively assigned the line 2665 seen by Cheo and Cooper [20] to the transition indicated. Humphreys [40] lists 2665, 2741, and 3050 as strong spontaneous lines. The nearest known line to 2649.41 is 2649.27, an  $f \rightarrow d$  transition [51]. Since the wavelength lies outside the error quoted by Cheo and Cooper and since other  $f \rightarrow d$  transitions have not been observed, this identification seems unlikely.

The lines listed as appearing in the discharge afterglow (4318, 4387, 4583, 4695, and 5125) were obtained in a mixture of helium and krypton by Laures, Dana, and Frapard [17], [19]. Laser oscillation lasting a few microseconds was observed several microseconds after the end of the excitation pulse; Laures and Dana [19] postulate that excitation takes place by collisions of the second kind between krypton ions and metastable helium atoms:



+ He(0) + kinetic energy.

The lower levels for all these lines are the upper levels of laser lines observed in pure krypton, with the exception of the line 4695, which ends on the upper level of one of the strongest spontaneous lines, 4355.47 [51]. Thus a mechanism exists to depopulate the lower levels rapidly enough to obtain a population inversion. The presence of 10 torr of helium in the discharge was apparently responsible for the suppression of the electron-collision-excited lines observed in pure krypton by others. Peak output power of 5W was reported for the strongest lines [17].

The line 4650.16 may actually have been C III (Table XI), although the krypton assignment is not unreasonable. Two new Kr II lines, 5022 and 5753, are reported by Bell and Bloom [9]. The errors estimated for the wavelength measurement of the lines at 6764 and 6871 have been revised upward by Bridges and Chester after a re-examination of their spectrographic plates; the original classification is unchanged, however. Humphreys records the line 8588 as a moderately strong line in spontaneous emission and assigns it to Kr III [40].

Continuous operation was reported for an unspecified number of Kr II lines [10]; the several lines indicated (cw) in Table IV were obtained with short discharge lengths (20 cm) and modest input powers (3 kW or less) [46]. It is likely that other Kr II lines will oscillate in longer tubes or with more input power. No accurate measurement of the gain of any of the strong Kr II lines has been reported; the authors' experience is that the gains are considerably less than the strongest Ar II lines and are probably 1 or 2 dB/m at most.

Table V: Xenon

More ion laser lines have been obtained in xenon to date than in any other gas. It is fortunate that good line

lists exist [40], [52]–[54] for Xe II and Xe III, although, from the number of unclassified and partially identified levels found in Table V, it is clear that more work is needed.

A possible assignment for the line 2477 is Xe III  $6p\ ^3P_0 \rightarrow 5d\ ^5D_1^0$ , 2477.04, as calculated from tabulated energy levels [36]; the authors could not find this line listed in spontaneous emission, however. Cheo and Cooper [20] list the line 2691.82 as xenon, while an unclassified line 2691.86 appears in Humphreys' krypton list [40]. Considering the difficulties of contamination in this kind of work, the actual source of this line is still undetermined. The line 2984 reported by Bridges and Chester as xenon [13] is most likely the strong oxygen line 2983.78; this line favored relatively higher xenon pressures than other oxygen impurity or xenon lines, so that xenon listing remains a possibility. The line 3079.71 is attributed to Xe II by Minnhagen (private communication to Cheo and Cooper); the authors' assignment to Xe IV is based on the similarity in time behavior to the Ar IV lines, i.e., a short laser burst at the peak of the highest obtainable discharge current. Dana, Laures, and Rocherolles have assigned this line to Ne III  $3p''\ ^3P_0 \rightarrow 3s''\ ^1P_1^0$ , 3078.86; from the sequence of gas mixtures used in their experiments [22], it seems likely that the xenon assignment is appropriate for their observation also.

Cheo and Cooper's measurement accuracy on the line 3305.92 rules out our previous assignment of this line to  $nx37_{3,2} \rightarrow 6p'\ ^3D_2$ , 3306.53 [13]. The assignment to Xe III, IV is again from Minnhagen (private communication). The lines 3483, 3645, 3803, and 3973 do not appear in the older literature (e. g., Kayser [43] or Humphreys [40]), although it is quite possible that the discharge configuration and current densities used for laser operation are capable of exciting previously unobserved lines.

The lines 4603, 5262, and 5419 dominate the blue-green region with modest excitation currents ( $100\ \text{\AA}/\text{cm}^2$ ); at higher currents (and especially with shorter pulses  $\approx 10\ \mu\text{s}$ ) the group of lines 4954, 5008, 5159, 5353, and 5395 dominates. These five lines are tentatively assigned to Xe III because of their higher current thresholds. This assignment also agrees with Humphreys' observed excitation dependence [40]. Heard and Peterson [30] report five other lines (not listed in Table V) at approximately the same relative positions in the xenon spectrum, but with somewhat different wavelengths. Their wavelength measurement error is sufficiently great that the five lines are quite likely the same five unclassified lines observed by the authors [32].

The lines listed as afterglow lines, 4862, 5314, 5727, and 6094, were obtained by Laures, Dana, and Frapard in a neon-xenon plasma [18], [19]. As in the case of the helium-krypton afterglow lines, they postulate a collisional transfer excitation of the upper laser level.

$\text{Ne}(3s\frac{3}{2}) + \text{Xe}^+(0) \rightarrow \text{Ne}(0)$

+  $\text{Xe}^+(7s\ ^4P_{3/2,5/2})$  + kinetic energy.

This excitation mechanism is undoubtedly correct for the three lines with 7s upper levels. The line 5727 is incorrectly identified in [19]; the  $p' \rightarrow d'$  assignment listed in Table V is given by Humphreys, et al. [54] determined from the observed Zeeman pattern, although the assignment given by Dana and Laures [19] appears as an alternate in the earlier work [53]. The  $p' \rightarrow d'$  assignment is also consistent with the observation of this line in a pure xenon discharge by Bell and Bloom [9]. Excitation of this line in a neon-xenon mixture in which all the pure xenon  $p \rightarrow s$  and  $p \rightarrow d$  laser transition are missing is likely due to the near-resonance of its upper level  $6p'\ ^2D_{5/2}$  at  $132,207.68\ \text{cm}^{-1}$  with the upper level of the strong collisionally excited laser line 5314,  $7s\ ^4P_{5/2}$ , at  $132,518.7\ \text{cm}^{-1}$ . We propose that the  $6p'$  level is populated from the 7s level by collisional transfer. Dana has observed competition between these two lines, with suppression of 5314 being necessary to obtain oscillation at 5727 [55].

The infrared lines marked (\*) should be interpreted as the strongest lines within the group reported by Sinclair [21]; relative strengths between these and the visible lines are not known. The line 9265 is somewhat surprising because it is a  $d \rightarrow p$  transition with a change of core, change of spin, and  $\Delta J \neq \Delta L$ . However, its lower level is the upper level of the strong line 5419.

#### Table VI: Chlorine

All observations to date on ionized chlorine are from McFarlane [16], [27]. The observed values for the lines 4905 and 4918 differ from the values calculated from the wavelength tables [36] by more than the estimated error. McFarlane points out, however, that the observed values for these lines listed in the MIT tables [48], 4904.76 and 4917.72, also differ from the calculated values [27].

Pulsed oscillation on the lines 5218, 5221, and 5392 was obtained in a 7-mm diameter by 1-m-long cold cathode tube with 20 to 50 m Torr of pure chlorine and 500-A peak discharge current. The remaining lines were observed with a 3-mm  $\times$  0.5-m tube and peak currents of less than 60 A. The threshold of the line 5218 was reduced to 1 A in this tube by adding 0.8 Torr of neon to 20 m Torr of chlorine; under these conditions some of the other Cl II lines were suppressed. To obtain all nine lines in the 3-mm tube, the neon partial pressure had to be reduced to 0.3 Torr, which raised the 5218 threshold to 8 A [27].

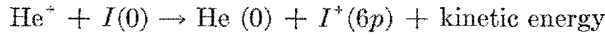
Continuous operation was obtained on the line 5218 by using 0.5 Torr of chlorine in a 1-mm bore tube. The observed current threshold was considerably less than 3 A, and operation for 10 to 15 seconds was obtained before cathode failure [27].

#### Table VII: Iodine

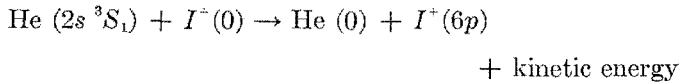
Fowles and Jensen have done all the work reported to date on ionized iodine [14], [15], [25]. Twelve lines have been obtained. (The line 5419 in [25] has been omitted from this table since it is most likely the strong Xe II

line; xenon had been used in the same discharge tube, and the line was not reproducible in iodine [26]). Following Fowles and Jensen, we have used the paper by Martin and Corliss [39] for wavelengths and identifications, since this later work corrects the I II spectrum given in *Atomic Energy Levels* [36].

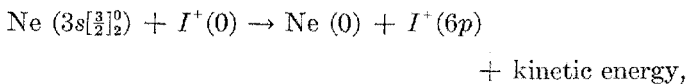
All I II lines were observed to oscillate only in the discharge afterglow. Typical operating conditions were a few Torr of helium and 0.1-Torr vapor pressure of iodine in a 5-mm diameter by 1.2-m long cold cathode discharge, although different pressure and excitation conditions were necessary to produce oscillation on several lines [25]. Fowles and Jensen have proposed that the process



is responsible for populating the upper laser levels [15]. However, oscillation was also obtained at 5626 and 6095 in a neon-iodine discharge and at 6095 in a krypton-iodine discharge. No oscillation could be obtained with argon or xenon as buffer gases [25]. Both helium and neon metastable states have sufficient energy to excite an iodine ion by a process analogous to that reported for krypton and xenon by Laures, et al. [17]–[19]:



or



with the iodine ion having been created by a prior collision with another helium or neon metastable. Argon and the heavier noble gases do not possess sufficiently energetic metastables to excite the iodine ion ground state. The existence of oscillation in a krypton-iodine discharge but not in an argon-iodine discharge is, indeed, puzzling.

Fowles reports gains of 3 to 5 per cent/m estimated from mirror transmission curves and power outputs of 0.1 to 0.5 mW for the stronger lines [26].

The four infrared lines around one micron reported in [25] are assumed by Fowles and Jensen to arise from neutral iodine because of their much longer time delay in the afterglow; accordingly, they are not listed here.

#### Table VIII: Oxygen

Sixteen oxygen ion lines have been observed to oscillate. Several of these are quite strong and are readily seen as impurities in other discharges. The set of four strong lines 4347, 4351, 4415, and 4417 may well find technological application if cathodes can be made which work well in an oxygen environment.

The line 2984 was incorrectly assigned by Bridges and Chester [13], and this error was called to our attention by Cooper [56]. We originally listed the line 3047 as an Ar II  $f \rightarrow d'$  line [13]; Cheo and Cooper's more accurate measurements rule out this assignment and furthermore

establish its identity as a relatively persistent oxygen line [56].

The authors observed oxygen laser lines only as impurities in noble gas discharges, and therefore we can say little about optimum excitation conditions, except that they are rather uncritical and the lines oscillate strongly at low oxygen partial pressures. McFarlane used a 7-mm diameter by 1-m long cold-cathode tube, with gas pressures of 20 to 50 m Torr and discharge currents in excess of 500 A [12]; some of his measurements have been repeated in a 3-mm-diameter tube [27]. Cheo and Cooper used 4-mm and 2-mm diameter by 1-m-long, cold-cathode tubes with gas pressures of 1 to 100 m Torr, and discharge currents up to 2000 A. Continuous operation has not yet been reported for oxygen.

#### Table IX: Nitrogen

The same discharge tubes and excitation conditions were used by McFarlane [12] and Cheo and Cooper [20] for nitrogen as just described for oxygen. Heard and Peterson [31] report a number of lines in a mercury-nitrogen discharge in the blue and green region, but again their wavelength measurements are not sufficiently accurate to distinguish them from or assign them to the lines listed in Table IX [32].

Continuous operation has not been reported for nitrogen, although Heard and Peterson report 500- $\mu$ s-laser output pulse lengths for the 5679 line with 150 A discharge current [31].

#### Table X: Mercury

With the exception of the line 4797, all the observations of mercury ion laser action are from Bell, Bloom and Lopez [1], [7] and all occur in the afterglow of a helium-mercury discharge. The two Hg II visible lines 5678 and 6150 are both reported to have high gain, much greater than the 10–20 per cent/m originally reported [1]. Super-radiance has been observed at 6150, implying a gain comparable to the stronger lines in the noble gases [9]. Peak output power reported [1] was 40 W. A cold cathode discharge tube of 15-mm diameter by 2.25 m long was used for the spectroscopic work reported in [7]. The lines listed were produced with a few m Torr pressure of mercury vapor and about 1-Torr helium; discharge currents up to 50 A were used.

It is interesting that all the well-identified levels involved in laser action have  $J = L + S$  and consequently only one line of each multiplet oscillates. This contrasts sharply with the situation for all the other observed ion laser gases, which may have several members of the same multiplet oscillating. Also, the mixture of transition  $p \rightarrow s$ ,  $p \rightarrow d$ ,  $d \rightarrow p$ ,  $f \rightarrow d$ ,  $s \rightarrow p$ ,  $g \rightarrow f$  is not observed in other gases. Bloom, Bell, and Lopez [7] speculate that the upper laser levels are populated from the mercury neutral ground state by direct electron collision. The occurrence of the laser pulse in the discharge afterglow seems to argue for a collisional transfer process analogous

to those proposed for the afterglow lines of krypton, xenon, and iodine. The two visible lines have also been obtained with neon [9], [46] and argon [9], [29] as buffer gases.

The Hg III line 4797 observed by Gerritsen and Goedertier [8] behaves more like the "pure gas" ion lasers, which make up the majority of the lines obtained so far. They used a 6-mm diameter by 1.2-m-long tube, with a mercury pool cathode. Oscillation was obtained with the surprisingly low pulse current of 5 A (compared with the larger values used to obtain the multiply ionized noble and atmospheric gases) and occurred during the current pulse. Oscillation of the 5678 and 6150 lines was obtained in the same tube, which originally contained 0.5 Torr of helium, but Gerritsen and Goedertier report that the 4797 line was obtained only after substantial cleanup of the helium. The more accurate measurement ( $\pm 0.1 \text{ \AA}$ ) listed for this line confirms the original assignment [57]. Continuous operation has not been reported for any of the mercury lines; however, Bell reports that the visible lines 4797, 5678, and 6150 are also observed in a pure mercury discharge [9].

*Table XI: Miscellaneous*

Oscillation on the very strong (spontaneous emission) Si IV line at 4089 was recorded on a spectrographic plate only once. Although this line was not reproducible, the conditions under which it appeared were conducive to the production of free silicon in the discharge region; namely, very low gas pressure (xenon) and very high currents, which produced erosion and "sparking" of the quartz discharge tube walls near constrictions [46].

The two C III lines are from McFarlane [12], who used CO<sub>2</sub> as the discharge gas. He reports that the C III lines then persisted in a pure O<sub>2</sub> discharge. The authors observed the line 4647 in krypton, xenon, and air discharges into which no carbon was intentionally introduced. Heard and Peterson [31] report a line at 4650 obtained in CO but not in CO<sub>2</sub> or other gases [32]. Unfortunately, their wavelength measurements are not sufficiently accurate to determine whether it is the same line as either of the two listed here.

The three infrared lines listed have been reported by Heard, Makhov, and Peterson [28], [29] in a mercury-argon discharge and are attributed to argon by Heard [32]. Although they are not definitely known to be ion lines, they were observed under conditions that produced oscillation on the visible Ar II and Hg II lines [29]. It is possible, however, that two of these may be the strong neutral argon lines observed by McFarlane [27]:

$$\begin{aligned} 12403 \text{ \AA} & \quad 3d\left[\frac{3}{2}\right]_1^0 \rightarrow 4p\left[\frac{3}{2}\right]_1 \\ 12703 \text{ \AA} & \quad 3d\left[\frac{3}{2}\right]_1^0 \rightarrow 4p'\left[\frac{1}{2}\right]_1. \end{aligned}$$

The remaining four lines 3760, 4645, 4650.40, and 6577 are lines that were observed only once (in the case of the first three) or for which the gas of origin was seriously in doubt (6577).

DISCUSSION

On the basis of the tables given in the preceding section, we may draw a number of conclusions concerning the conditions for laser action in ions. The classified transitions tabulated in Table II through XI may generally be grouped in three categories: "normal" lines, involving  $p \rightarrow s$  and  $p \rightarrow d$  transitions among the lowest excited ionic levels; "reverse" lines, of the form  $d \rightarrow p$ , arising from more highly excited levels; and lines of all kinds occurring in the afterglow, apparently populated by resonant atom-atom collisions directly or by subsequent cascading.

A characteristic common to all three groups is that the strongest laser lines are also the strong lines observed in spontaneous emission. Where uniformly measured spectroscopic line intensities are available (see, e.g., [38]), this property is quite evident. For atomic energy levels falling within the framework of the  $L$ - $S$  coupling approximation, this observed characteristic suggests that the strongest laser lines should satisfy the preferred  $L$ - $S$  coupling rules,  $\Delta J = \Delta L$ , especially  $\Delta J = \Delta L = +1$ , with no change in core or total spin (see, e.g., Condon and Shortley [59]). The summary in Table XII shows this property and, in addition, shows that the rule  $\Delta J = \Delta L$  has even wider applicability than the other  $L$ - $S$  coupling rules; about three-fourths of the transitions involving a core or spin change (forbidden in  $L$ - $S$  coupling) obey it.

Bridges and Chester have compared relative line strengths calculated from  $L$ - $S$  coupling with their observed laser lines in the singly and doubly ionized noble gases [13]. The agreement is not as good as that obtained in the similar calculation of Faust, et al. [60] for the transitions of neutral neon. On the other hand, we would not expect such good agreement since lines in different gases are compared, rather than different lines in the same gas, and only a restricted wavelength range has been studied. The more recent work of Cheo and Cooper [20] adds six lines to the comparison given in [13], with all the new lines falling in the "right" blocks. Horrigan, Koozekanani, and Paananen [23] have estimated absolute line strengths for a few of the Ar II transitions, using the  $L$ - $S$  coupling model with radial integrals evaluated under the Coulomb approximation of Bates and Dangaard [61] and the Hartree-Fock approximation. Their results agree with the lifetimes measured by Bennett, et al. [33] and help explain why only one  $4p \rightarrow 3d$  line (the one at  $1.09\mu$ ) was observed in Ar II.

A more general coupling model is necessary to treat transitions that violate the  $L$ - $S$  coupling rules, for example, the very strong line Ar II 5145, which has a spin change, or the four Ar II  $4p' \rightarrow 3d$  lines, which suffer core changes. Calculations utilizing an intermediate coupling scheme are being made by Statz, Tang, and Horrigan [62]. In general, it is expected that  $J_c - l$  coupling will prove to give a more appropriate description of laser lines originating from states of higher energy [38], or in the heavier gases [59] such as krypton and xenon.

A recent report by Griem [63] tabulates calculated oscillator strengths for selected visible and ultraviolet transitions in the lighter elements (up to and including argon) in various ionization states. Several ion laser lines are included in the list. Griem's calculations are also based on Bates' and Damgaard's Coulomb approximation [61].

The relevant processes for the "normal"  $p \rightarrow s$ ,  $p \rightarrow d$  transitions are reasonably clear, although there seem to be two population processes at work; direct electron excitation and stepwise electron excitation. It is probable that their regions of occurrence overlap.

Bennett, et al. [5] have proposed direct electron excitation from the neutral atom ground state to the upper state to the upper laser level as the dominant populating mechanism. The preponderance of laser lines with  $p$  upper states follows from the selection rules of the "sudden perturbation" process referred to by Bennett. The short radiative lifetimes of the  $s$  and  $d$  lower levels then guarantee an inversion. From the evidence available at the present time, it seems likely that this population mechanism is dominant only in pulsed discharges with high  $E/p$  and short pulse duration. This excitation mechanism should yield a linear dependence with discharge current of the spontaneous emission from the upper laser level and a square-to-linear dependence for the output power (depending on level of saturation). Such a current dependence has not been reported (although Cheo and Cooper [20] report linear regions in a rather complex overall behavior; see following paragraph).

McFarlane [12] has extended this argument to the transitions in oxygen and nitrogen. He points out that, for levels in the higher degrees of ionization, the excitation must be from a lower degree *ion* ground state with the appropriate parity, not the neutral ground state, so that at least two steps are necessary for excitation. This later observation is consistent with McFarlane's [27] and Cheo and Cooper's [20] observations that the higher ionization states oscillate more readily in large diameter tubes, where the effect on ion recombination at the wall is smaller. It is also consistent with Cheo and Cooper's observed current dependence of oscillation in different ionization states, namely, that the doubly ionized lines appear after saturation of the singly ionized lines, the triply ionized lines appear after saturation of the doubly ionized lines and decline of the singly ionized lines, and so forth [20]. The simultaneous occurrence of atoms with different degrees of ionization complicates the current dependence and makes it difficult to draw conclusions on this basis.

In the case of continuous operation there is little doubt that the upper laser levels are populated by a two-step process<sup>2</sup>: an electron collision to produce ionization, fol-

lowed by an electron collision to excite the upper laser level [10], [35]. One might expect this stepwise process to yield a higher population of lower laser levels ( $s$  and  $d$  states) since they are of opposite parity to the ionic ground state. However, it is just this relationship that gives the lower levels their short lifetime. It is possible that the upper levels ( $p$  states) with the same parity as the ionic ground state may be populated in part by cascading from higher  $s$  or  $d$  states. This would also explain the few "reverse"  $d \rightarrow p$  lines that have been tentatively identified (although none of these have yet been observed in continuous operation). If cascading from higher  $s$  and  $d$  states were really the dominant process, however, we would expect to see a few  $f \rightarrow d$  laser transitions (in the noble gases); none have been observed to date. The conclusion is that the upper laser levels are populated directly from the ionic ground state.<sup>3</sup> A two-step process is necessary to yield the observed  $I^2$  dependence for the spontaneous emission from the upper levels [34] and the observed  $I^4$  to  $I^2$  (again, depending on the saturation) dependence for the output power [9], [10], [35], [46], [49]. A most detailed description of the evidence is given by Gordon, et al. [35] for Ar II.

The "reverse" lines observed in neon, argon, and xenon remain somewhat of a problem. None are particularly strong or are of "certain" identification. However, all share one common property, which makes their occurrence seem plausible, at least: strong spontaneous lines (and often laser lines) originate from their lower levels so that population inversion may occur by rapid lower level depletion. These lines could stand more study.

The mechanisms for the collisionally pumped lines have already been discussed under the individual gases. Resonant collisional pumping by metastable atoms is clearly the mechanism at work in the case of the Kr II and Xe II lines. We add only that Gordon and Labuda have observed a change in the relative strengths of the blue-green Ar II lines with the addition of helium, the changes being consistent with the picture of helium metastable collisional pumping of selected transitions [34]. The effect is not so striking as in helium-krypton or neon-xenon because the lines affected are the lines that oscillate in the absence of helium.

The particular species responsible for collisional pumping in the case of I II is less clearly determined. Whether collisional pumping even plays a role in the case of mercury is not known. More work is needed on these two gases and with other mixtures in which long-lived metastables may be used to pump the ionic transitions. The degree of coincidence between energy levels required to produce collisional transfer of excitation is apparently much less when one atom is ionized; it should be much easier to find sufficiently resonant systems.

<sup>2</sup> Only singly ionized lines have been observed in continuous operation; therefore, only two steps are necessary for stepwise excitation.

<sup>3</sup> There is also evidence that electron collision excitation from ionic metastables (e. g., the  $4s^1P$  levels in argon) may contribute to the upper-level population [34].

Calculated Wavelength	Classification	References
* Strong or characteristic line in pure gas.	? Classification uncertain.	cw Continuous oscillation reported.
? Existence of this line may be doubtful.	. . . Classification unknown.	D Disagrees with present paper.
A Reported in discharge afterglow only.	** Classification made by present authors on the basis of measured wavelength.	E Error in classification or wavelength.
[ ] Wavelength not calculated from Atomic Energy Levels; see reference indicated.		G Gain measured.
. . . No spectroscopic confirmation of this line.		P Output power reported.

Calculated Wavelength in Å (Air)	Best Measured Wavelength in Å (Air)	Classification	References
2357.96 [58]	2358.00 ± 0.06	IV $3p^4 D_{7/2}^o \rightarrow 3s^4 P_{5/2}$	20
2473.40 [41]	2473.50 ± 0.06	III . . .	20
2677.90	2677.98 ± 0.06	III $3p^3 P_{2,0} \rightarrow 3s^3 S_1^o$	13, 20
2678.64	2678.68 ± 0.06	III $3p^3 P_1 \rightarrow 3s^3 S_1^o$	13, 20
2777.65	2777.5 ± 0.5	III $(^2D^o) 3p^3 D_3 \rightarrow (^2D^o) 3s^3 D_3^o$	13
. . .	2866.88 ± 0.06	IV? . . .	13, 20
3319.75	3319.84 ± 0.06	II $(^1D) 3p^2 P_{1/2}^o \rightarrow (^1D) 3s^2 D_{3/2}$	20, 22
* 3323.77	3323.79 ± 0.06	II $3p^2 P_{3/2}^o \rightarrow 3s^2 P_{3/2}$	13, 20, 22
. . .	3324.37 ± 0.1	. . .	22
? 3327.17	3327.5 ± 0.5	II $3p^4 D_{3/2}^o \rightarrow 3s^4 P_{3/2}$	13
3329.23	3329.02 ± 0.1	II $3d^4 D_{7/2} \rightarrow 3p^4 D_{7/2}^o$	22
3331.14	3331.07 ± 0.1	III $(^2P^o) 3p^3 D_2 \rightarrow (^2P^o) 3s^1 P_1^o$	22
3345.52	3345.50 ± 0.06	II $(^1D) 3p^2 P_{3/2}^o \rightarrow (^1D) 3s^2 D_{5/2}$	20, 22(E)
* 3378.30	3378.33 ± 0.06	II $3p^2 P_{1/2}^o \rightarrow 3s^2 P_{1/2}$	13, 20, 22
* 3392.86	3392.86 ± 0.06	II $3p^2 P_{3/2}^o \rightarrow 3s^2 P_{1/2}$	13, 20
3393.20	3393.40 ± 0.1	II $3d^2 D_{3/2} \rightarrow 3p^2 D_{5/2}^o$	22

TABLE III		ARGON		
Calculated Wavelength in Å (Air)	Best Measured Wavelength in Å (Air)		Classification	References
2624.93	2624.90 ± 0.06	IV	$(^1D) 4p \ ^2D_{5/2}^o \rightarrow (^1D) 4s \ ^2D_{5/2}$	20
2753.92 [42]	2753.91 ± 0.06	III	. . .	13, 20
2884.16	2884.24 ± 0.06	III	$(^2D^o) 4p \ ^3P_2 \rightarrow (^2D^o) 4s \ ^3D_3^o$	20, 22
2913.00	2912.92 ± 0.06	IV	$4p \ ^2D_{5/2}^o \rightarrow 4s \ ^2P_{3/2}$	13, 20, 22
2926.27	2926.24 ± 0.06	IV	$4p \ ^2D_{3/2}^o \rightarrow 4s \ ^2P_{1/2}$	13, 20, 22
3002.66 [42]	3002.64 ± 0.06		. . .	13, 20, 22(E)
3024.05	3024. ± 0.5	III	$(^2P^o) 4p \ ^3D_3 \rightarrow (^2P^o) 4s \ ^3P_2^o$	13
3054.84	3054.8 ± 0.5	III	$(^2P^o) 4p \ ^3D_2 \rightarrow (^2P^o) 4s \ ^3P_1^o$	13
3336.13	3336.14 ± 0.1	III	$(^2D^o) 4p \ ^3F_4 \rightarrow (^2D^o) 4s \ ^3D_3^o$	13, 20, 22
3344.72	3344.78 ± 0.1	III	$(^2D^o) 4p \ ^3F_3 \rightarrow (^2D^o) 4s \ ^3D_2^o$	13, 20, 22
3358.49	3358.52 ± 0.06	III	$(^2D^o) 4p \ ^3F_2 \rightarrow (^2D^o) 4s \ ^3D_1^o$	13, 20, 22
* 3511.12	3511.13 ± 0.06	III	$4p \ ^3P_2 \rightarrow 4s \ ^3S_1^o$	13, 16, 20, 22
3514.18	3514.15 ± 0.06	III	$4p \ ^3P_1 \rightarrow 4s \ ^3S_1^o$	13, 16, 22
3576.61 [38]	3576.9 ± 0.5	II	$4d \ ^4F_{7/2}^o \rightarrow 4p \ ^4D_{5/2}$	13
3637.89 [48]	3637.86 ± 0.04	III	$(^2D^o) 4p \ ^1F_3 \rightarrow (^2D^o) 4s \ ^1D_2^o$	13, 16, 20, 22
. . .	3705.2 ± 0.5	III?	. . .	13
3795.32	3795/28 ± 0.06	III	$(^2P^o) 4p \ ^3D_3 \rightarrow (^2P^o) 3d \ ^3P_2^o$	13, 22
3858.29	3858.26 ± 0.06	III	$(^2P^o) 4p \ ^3D_2 \rightarrow (^2P^o) 3d \ ^3P_1^o$	13
4146.71	4146.60 ± 0.04	III	$(^2D^o) 4p \ ^3P_2 \rightarrow (^2P^o) 4s \ ^3P_2^o$	13
* 4182.98 [42]	4182.92 ± 0.06	III?	. . .	13
4370.75	4370.73 ± 0.06	II	$(^1D) 4p \ ^2D_{3/2}^o \rightarrow 3d \ ^2D_{3/2}$	13
4481.81	4482	II	$(^1D) 4p \ ^2D_{5/2}^o \rightarrow 3d \ ^2D_{5/2}$	9
4545.05 [38]	4545.04 ± 0.1	II	$4p \ ^2P_{3/2}^o \rightarrow 4s \ ^2P_{3/2}$	2(G, P), 4, 10 (cw, P), 13
* 4579.35 [38]	4579.36 ± 0.16	II	$4p \ ^2S_{1/2}^o \rightarrow 4s \ ^2P_{1/2}$	2(P), 4, 5(G), 10 (cw, P), 13, 29
4609.56 [38]	4609.57 ± 0.1	II	$(^1D) 4p \ ^2F_{7/2}^o \rightarrow (^1D) 4s \ ^2D_{5/2}$	13
4657.89	4657.95 ± 0.02	II	$4p \ ^2P_{1/2}^o \rightarrow 4s \ ^2P_{3/2}$	2(P), 4, 5(G), 10 (cw, P), 13
4726.86 [38]	4726.89 ± 0.04	II	$4p \ ^2D_{3/2}^o \rightarrow 4s \ ^2P_{3/2}$	2(P), 10(cw, P), 13

TABLE III

## ARGON (CONTINUED)

Calculated Wavelength in Å (Air)	Best Measured Wavelength in Å (Air)	Classification	References
* 4764.86	4764.88 ± 0.04	II $4p^2 P_{3/2}^o \rightarrow 4s^2 P_{1/2}$	2(P), 3(E,G), 4(G), 5(G,P), 10(cw,P), 13, 29
* 4879.86	4879.86 ± 0.04	II $4p^2 D_{5/2}^o \rightarrow 4s^2 P_{3/2}$	2(E,G,P), 4(G), 5(G,P), 10(cw,P), 13 (G), 29(E)
4889.03	4889.06 ± 0.06	II $4p^2 P_{1/2}^o \rightarrow 4s^2 P_{1/2}$	13, 24
* 4965.07	4965.09 ± 0.02	II $4p^2 D_{3/2}^o \rightarrow 4s^2 P_{1/2}$	2(P), 4, 5(G,P), 10 (cw,P), 13, 29
4992.8 [43]	4992.55 ± 0.05	III?	24
* 5017.16 [38]	5017.17 ± 0.02	II $(^1D) 4p^2 F_{5/2}^o \rightarrow 3d^2 D_{3/2}$	2(P), 4(E), 5(G,P), 10 (cw,P), 13
5141.79 [38]	5141.8 ± 0.05	II $(^1D) 4p^2 F_{7/2}^o \rightarrow 3d^2 D_{5/2}$	13, 24
* 5145.32 [38]	5145.33 ± 0.02	II $4p^4 D_{5/2}^o \rightarrow 4s^2 P_{3/2}$	2(G,P), 4(G), 5(G,P), 10(cw,P), 13, 29
5286.90 [38]	5287. ± 1	II $4p^4 D_{3/2}^o \rightarrow 4s^2 P_{1/2}$	2(P), 10(cw,P), 13
5502.20	5502.2 ± 0.5	III $(^2D^o) 4p^3 D_3 \rightarrow (^2P^o) 4s^3 P_2^o$	13, 24
8771.86	8780. ± 3	** II $4p^2 P_{3/2} \rightarrow (^1D) 4s^2 D_{5/2}$	21
* 10923.44 [38]	10923. ± 1	II $4p^2 P_{3/2}^o \rightarrow 3d^2 D_{5/2}$	21, 23(P), 46(cw)

TABLE IV

## KRYPTON

Calculated Wavelength in Å (Air)	Best Measured Wavelength in Å (Air)	Classification	References
. . . .	2649.41 ± 0.06	. . . .	20
2664.41	2664.50 ± 0.06	** II $(^1D) 5d^2 P_{3/2} \rightarrow 5p^4 D_{1/2}$	20
2741.39 [40]	2741.51 ± 0.06	. . . .	20
3049.70 [40]	3049.74 ± 0.06	. . . .	13, 20
3124.38	3124.43 ± 0.06	III $(^2D^o) 5p^1 D_2 \rightarrow (^2D^o) 5s^1 D_2^o$	20
3239.51	3239.43 ± 0.06	III $(^2P^o) 5p^1 D_2 \rightarrow (^2P^o) 5s^1 P_1^o$	13, 20
3374.96	3375.0 ± 0.5	III $(^2P^o) 5p^3 D_3 \rightarrow (^2P^o) 5s^3 P_2^o$	13
* 3507.42	3507.42 ± 0.06	III $5p^3 P_2 \rightarrow 5s^3 S_1^o$	13, 20
3564.23	3564.20 ± 0.06	III $5p^3 P_1 \rightarrow 5s^3 S_1^o$	20
* 4067.37	4067.36 ± 0.06	III $(^2D^o) 5p^1 F_3 \rightarrow (^2D^o) 5s^1 D_2^o$	13
* 4131.33	4131.38 ± 0.06	III $5p^5 P_2 \rightarrow 5s^3 S_1^o$	13
4154.44	4154.45 ± 0.04	III $(^2D^o) 5p^3 F_3 \rightarrow (^2D^o) 5s^1 D_2^o$	13

TABLE IV		KRYPTON (CONTINUED)		
Calculated Wavelength in Å (Air)	Best Measured Wavelength in Å (Air)	Classification		References
4171.79	4171.81 ± 0.1	III	5p <sup>3</sup> P <sub>1</sub> → 5s <sup>3</sup> S <sub>1</sub> <sup>o</sup>	13
4226.58	4226.51 ± 0.06	III	( <sup>2</sup> D <sup>o</sup> ) 5p <sup>3</sup> F <sub>2</sub> → ( <sup>2</sup> D <sup>o</sup> ) 4d <sup>3</sup> D <sub>1</sub> <sup>o</sup>	13
A 4317.81	4318	II	6s <sup>4</sup> P <sub>5/2</sub> → 5p <sup>4</sup> P <sub>5/2</sub> <sup>o</sup>	17(P), 19
A 4386.54	4387	II	6s <sup>4</sup> P <sub>5/2</sub> → 5p <sup>4</sup> P <sub>3/2</sub> <sup>o</sup>	17(E), 19(E)
4443.29	4443.28 ± 0.04	III	( <sup>2</sup> D <sup>o</sup> ) 5p <sup>3</sup> D <sub>2</sub> → ( <sup>2</sup> D <sup>o</sup> ) 4d <sup>3</sup> D <sub>1</sub> <sup>o</sup>	13
4577.20	4577.20 ± 0.1	II	( <sup>1</sup> D) 5p <sup>2</sup> F <sub>7/2</sub> <sup>o</sup> → ( <sup>1</sup> D) 5s <sup>2</sup> D <sub>5/2</sub>	6(G), 13
A 4582.85	4583	II	6s <sup>4</sup> P <sub>3/2</sub> → 5p <sup>4</sup> D <sub>5/2</sub> <sup>o</sup>	17, 19
* 4619.15	4619.17 ± 0.1	II	5p <sup>2</sup> D <sub>5/2</sub> <sup>o</sup> → 5s <sup>2</sup> P <sub>3/2</sub>	6(G), 13, 46(cw)
4633.86	4633.92 ± 0.06	II	( <sup>1</sup> D) 5p <sup>2</sup> F <sub>5/2</sub> <sup>o</sup> → ( <sup>1</sup> D) 5s <sup>2</sup> D <sub>3/2</sub>	6(G), 13
? 4650.16	4650.16 ± 0.1	II	5p <sup>2</sup> P <sub>1/2</sub> <sup>o</sup> → 5s <sup>4</sup> P <sub>1/2</sub>	13
* 4680.41	4680.45 ± 0.06	II	5p <sup>2</sup> S <sub>1/2</sub> <sup>o</sup> → 5s <sup>2</sup> P <sub>1/2</sub>	6(G), 13, 46(cw)
A 4694.44	4695	II	6s <sup>4</sup> P <sub>5/2</sub> → 5p <sup>4</sup> D <sub>7/2</sub> <sup>o</sup>	17(P), 19
* 4762.43	4762.44 ± 0.06	II	5p <sup>2</sup> D <sub>3/2</sub> <sup>o</sup> → 5s <sup>2</sup> P <sub>1/2</sub>	6(G), 13
4765.73	4765.71 ± 0.1	II	5p <sup>4</sup> D <sub>5/2</sub> <sup>o</sup> → 5s <sup>4</sup> P <sub>3/2</sub>	6(G), 13, 46(cw)
* 4825.17	4825.18 ± 0.06	II	5p <sup>4</sup> S <sub>3/2</sub> <sup>o</sup> → 5s <sup>2</sup> P <sub>1/2</sub>	6(G), 13
4846.59	4846.66 ± 0.06	II	5p <sup>2</sup> P <sub>1/2</sub> <sup>o</sup> → 5s <sup>2</sup> P <sub>3/2</sub>	13, 46(cw)
5022.40	5022	II	5p <sup>4</sup> D <sub>3/2</sub> <sup>o</sup> → 5s <sup>2</sup> P <sub>3/2</sub>	9
A 5125.73	5126	II	6s <sup>4</sup> P <sub>3/2</sub> → 5p <sup>4</sup> D <sub>3/2</sub> <sup>o</sup>	17, 19
5208.31	5208.32 ± 0.04	II	5p <sup>4</sup> P <sub>3/2</sub> <sup>o</sup> → 5s <sup>4</sup> P <sub>3/2</sub>	6(G), 13, 46(cw)
5308.65	5308.68 ± 0.04	II	5p <sup>4</sup> P <sub>5/2</sub> <sup>o</sup> → 5s <sup>4</sup> P <sub>3/2</sub>	6(G), 13, 46(cw)
* 5681.88	5681.92 ± 0.04	II	5p <sup>4</sup> D <sub>5/2</sub> <sup>o</sup> → 5s <sup>2</sup> P <sub>3/2</sub>	6(G), 13, 46(cw)
5752.98	5753	II	5p <sup>4</sup> D <sub>3/2</sub> <sup>o</sup> → 5s <sup>2</sup> P <sub>1/2</sub>	9
* 6470.88	6471.0 ± 0.5	II	5p <sup>4</sup> P <sub>5/2</sub> <sup>o</sup> → 5s <sup>2</sup> P <sub>3/2</sub>	6(G), 13
6570.12	6570.0 ± 0.5	II	( <sup>1</sup> D) 5p <sup>2</sup> D <sub>5/2</sub> <sup>o</sup> → 4d <sup>2</sup> F <sub>5/2</sub>	6(G), 13
6764.42	6764.57 ± 0.1	II	5p <sup>4</sup> P <sub>1/2</sub> <sup>o</sup> → 5s <sup>2</sup> P <sub>1/2</sub>	6(G), 13
6870.84	6870.96 ± 0.1	II	( <sup>1</sup> D) 5p <sup>2</sup> F <sub>5/2</sub> <sup>o</sup> → 4d <sup>2</sup> P <sub>3/2</sub>	6(G), 13
7993.22	7993.0 ± 0.5	II	5p <sup>4</sup> P <sub>3/2</sub> <sup>o</sup> → 4d <sup>4</sup> D <sub>1/2</sub>	6(G), 13, 21
8587.78 [40]	8589 ± 3	III	. . .	21

TABLE V

## XENON

Calculated Wavelength in Å (Air)	Best Measured Wavelength in Å (Air)	Classification	References
. . .	2477.18 ± 0.06	. . .	20
. . .	2691.82 ± 0.06	. . .	20
? 2983.85	2983.7 ± 0.5	III $(^2P^o) 6p 32_1 \rightarrow (^2P^o) 6s 3P^o_0$	13
3079.71 [40]	3079.78 ± 0.06	II, IV?	13, 20, 22(E)
3246.84	3246.94 ± 0.06	III $(^2P^o) 6p 3D_3 \rightarrow (^2D^o) 5d 3D^o_3$	20
3306.04 [44]	3305.92 ± 0.06	III, IV?	13(E), 20, 22(E)
3330.78 [40]	3330.82 ± 0.06	IV?	13, 20, 22(E)
3349.91 [44]	3350.04 ± 0.06	. . .	20
3454.24	3454.23 ± 0.06	III $(^2D^o) 6p 1D_2 \rightarrow (^2D^o) 6s 1D^o_2$	20, 22
. . .	3482.96 ± 0.06	. . .	13, 20
. . .	3645.46 ± 0.06	. . .	20, 22(E)
3669.15 [40]	3669.20 ± 0.06	. . .	20
3745.71	3745.73 ± 0.06	III $(^2D^o) 6p 1D_2 \rightarrow (^2D^o) 5d 1D^o_2$	20
3780.97	3780.99 ± 0.06	III $6p 3P_2 \rightarrow 6s 3S^o_1$	13, 20, 22
. . .	3803.27 ± 0.06	. . .	20
. . .	3972.93 ± 0.06	. . .	20
4060.41	4060.48 ± 0.06	III $(^2P^o) 6p 32_1 \rightarrow (^2P^o) 5d 25^o_1$	13, 22
4214.01	4214.05 ± 0.06	III $(^2D^o) 6p 3P_2 \rightarrow (^2D^o) 5d 3D^o_3$	13
4240.24	4240.26 ± 0.1	III $(^2D^o) 6p 1D_2 \rightarrow (^2P^o) 5d 17^o_3$	13
4272.59	4272.60 ± 0.06	III $(^2D^o) 6p 3F_4 \rightarrow (^2D^o) 5d 3D^o_3$	13
4285.88	4285.92 ± 0.06	III $(^2D^o) 6p 3D_3 \rightarrow (^2D^o) 6s 1D^o_2$	13
4305.85	4305.77 ± 0.06	III $(^2D^o) 6p 3D_3 \rightarrow (^2D^o) 5d 3D^o_3$	13
4434.15	4434.22 ± 0.1	III $(^2D^o) 6p 3F_2 \rightarrow (^2D^o) 5d 3D^o_1$	13
* 4603.03	4603.02 ± 0.04	II $6p 4D^o_{3/2} \rightarrow 6s 4P^o_{3/2}$	6(G), 9, 13, 46(cw)
4673.68	4673.73 ± 0.06	III $(^2D^o) 6p 1F_3 \rightarrow (^2D^o) 6s 1D^o_2$	13
4683.54	4683.57 ± 0.06	III $6p 5P_2 \rightarrow 6s 3S^o_1$	13
A 4862.49	4862	II $7s 4P^o_{5/2} \rightarrow 6p 4P^o_{5/2}$	18, 19
4869.46	4869.48 ± 0.06	III $(^2D^o) 6p 3F_3 \rightarrow (^2D^o) 5d 3D^o_2$	13

TABLE V		XENON (CONTINUED)	
Calculated Wavelength in Å (Air)	Best Measured Wavelength in Å (Air)	Classification	References
4887.30	4887	** II $6p^2 P_{3/2}^o \rightarrow 6s^2 P_{3/2}$	9
* 4954.16 [40]	4954.10 ± 0.06	III?	13
4965.08	4965.00 ± 0.06	II $(^1D) 7s^2 D_{3/2} \rightarrow (^1D) 6p^2 P_{3/2}^o$	9, 13
* 5007.78 [40]	5007.72 ± 0.04	III?	13
5044.92	5044.89 ± 0.06	II $(^1D) 6p^2 P_{1/2}^o \rightarrow (^1D) 6s^2 D_{3/2}$	6(G), 9, 13, 30, 46(cw)
* 5159.06 [40]	5159.04 ± 0.04	III?	13
5238.93	5238.89 ± 0.06	III $(^2D^o) 6p^3 P_2 \rightarrow (^2P^o) 5d 13_1^o$	13
5259.92	5260.17 ± 0.06	II $7s^4 P_{5/2} \rightarrow 6p^4 D_{5/2}^o$	13, 46
And 5260.43		II And $6p^2 P_{3/2}^o \rightarrow 6s^2 P_{1/2}$	13, 30, 46
5261.95	5261.5 ± 1	II $(^1D) 6p^2 D_{3/2}^o \rightarrow (^1D) 6s^2 D_{3/2}$	6(G), 9, 13, 30, 46(cw)
A 5313.87	5314	II $7s^4 P_{5/2} \rightarrow 6p^4 D_{7/2}^o$	18(G), 19
* 5352.88 [40]	5352.89 ± 0.06	III?	13
* 5394.59 [40]	5394.59 ± 0.06	III?	13
* 5419.15	5419.16 ± 0.06	II $6p^4 D_{5/2}^o \rightarrow 6s^4 P_{3/2}$	6(G), 9, 13, 26, 30, 46(cw)
5659.38	5659	** II $6p^2 P_{1/2}^o \rightarrow 5d^2 P_{1/2}$	9
A 5726.91	5727	** II $(^1D) 6p^2 D_{5/2}^o \rightarrow (^1D) 5d^2 F_{5/2}$	9, 19
5751.03	5751	** II $6p^2 D_{3/2}^o \rightarrow 5d^2 P_{1/2}$	9
5955.65 [40]	5955.73 ± 0.04	II?	13
* 5971.11	5971.12 ± 0.06	II $(^1D) 6p^2 P_{3/2}^o \rightarrow (^1D) 6s^2 D_{3/2}$	6(G), 9, 13, 30, 46(cw)
A 6093.61	6094	II $7s^4 P_{3/2} \rightarrow 6p^4 D_{3/2}^o$	19
6270.81	6270.90 ± 0.1	II $(^1D) 6p^2 F_{5/2}^o \rightarrow (^1D) 6s^2 D_{3/2}$	6(G), 9, 13, 30, 46(cw)
* 7827.63	7828 ± 3	II $35_5^o \rightarrow 16_{3/2}$	21
* 7988.00	7989 ± 3	II $6p^4 P_{1/2}^o \rightarrow 6s^4 P_{1/2}$	21
8332.70	8330 ± 3	II $27_5^o \rightarrow 6d^4 D_{5/2}$	21
8406.8 [40]	8408 ± 3	. . . .	21
8446.19	8443 ± 3	II $27_5^o \rightarrow 6d^4 D_{3/2}$	21
8566.7 [40]	8569 ± 3	. . . .	21
8582.51	8582 ± 3	II $31_3^o \rightarrow 10_{5/2}$	21

TABLE V		XENON (CONTINUED)		
Calculated Wavelength in Å (Air)	Best Measured Wavelength in Å (Air)		Classification	References
* 8716.17	8714 ± 3	II	$6p^4 D_{3/2}^{\circ} \rightarrow 5d^2 P_{3/2}$	21
* 9059.30	9063 ± 4	II	$27_{5/2}^{\circ} \rightarrow 16_{3/2}$	21
9265.39	9265 ± 4	II	$(^1S) 5d^2 D_{3/2} \rightarrow 6p^4 D_{5/2}^{\circ}$	21
9288.54	9287 ± 4	II	$13_{1/2}^{\circ} \rightarrow (^1D) 5d^2 S_{1/2}$	21
* 9698.59	9697 ± 4	II	$6p^4 D_{3/2}^{\circ} \rightarrow 5d^4 P_{5/2}$	21
10633.85	10634 ± 6	II	$6p^4 D_{3/2}^{\circ} \rightarrow 5d^4 P_{3/2}$	21
* . . . .	10950 ± 6		. . . .	21

TABLE VI		CHLORINE		
Calculated Wavelength in Å (Air)	Best Measured Wavelength in Å (Air)		Classification	References
4781.34	4781.34 ± 0.03	II	$(^2P^{\circ}) 4p^3 D_3 \rightarrow (^2P^{\circ}) 4s^3 P_2^{\circ}$	16, 27
4896.85	4896.88 ± 0.03	II	$(^2D^{\circ}) 4p^3 F_4 \rightarrow (^2D^{\circ}) 4s^3 D_3^{\circ}$	16, 27
4904.82	4904.73 ± 0.03	II	$(^2D^{\circ}) 4p^3 F_3 \rightarrow (^2D^{\circ}) 4s^3 D_2^{\circ}$	16, 27
4917.81	4917.66 ± 0.03	II	$(^2D^{\circ}) 4p^3 F_2 \rightarrow (^2D^{\circ}) 4s^3 D_1^{\circ}$	16, 27
5078.28	5078.30 ± 0.03	II	$(^2D^{\circ}) 4p^3 D_3 \rightarrow (^2D^{\circ}) 4s^3 D_3^{\circ}$	16, 27
* 5217.92	5217.90 ± 0.03	II	$4p^3 P_2 \rightarrow 4s^3 S_1^{\circ}$	16, 27(cw)
5221.35	5221.30 ± 0.03	II	$4p^3 P_1 \rightarrow 4s^3 S_1^{\circ}$	16, 27
5392.16	5392.15 ± 0.03	II	$(^2D^{\circ}) 4p^1 F_3 \rightarrow (^2D^{\circ}) 4s^1 D_2^{\circ}$	16, 27
6094.72	6094.74 ± 0.03	II	$(^2D^{\circ}) 4p^1 P_1 \rightarrow (^2D^{\circ}) 4s^1 D_2^{\circ}$	16, 27

TABLE VII		IODINE		
Calculated Wavelength in Å (Air)	Best Measured Wavelength in Å (Air)		Classification	References
A 4986.92 [39]	4986.	II	$(^2D^{\circ}) 6p^3 D_2 \rightarrow 5d^3 D_1^{\circ}$	25, 26(G, P)
A 5216.27 [39]	5216.	II	$(^2D^{\circ}) 6p^3 F_2 \rightarrow 5d^3 D_1^{\circ}$	25, 26(G, P)
*A 5407.36 [39]	5407.	II	$(^2D^{\circ}) 6p^3 D_2 \rightarrow (^2D^{\circ}) 6s^3 D_2^{\circ}$	15, 25, 26(G, P)
A 5625.69 [39]	5625.	II	$6p^3 P_2 \rightarrow 6s^3 S_1^{\circ}$	25, 26(G, P)

TABLE VII		IODINE (CONTINUED)		
Calculated Wavelength in Å (Air)	Best Measured Wavelength in Å (Air)	Classification		References
A 5678.08 [39]	5678.	II	$(^2D^o) 6p \ ^3F_2 \rightarrow (^2D^o) 6s \ ^3D_2^o$	15, 25, 26(G, P)
*A 5760.78 [39]	5760.	II	$(^2D^o) 6p \ ^3D_2 \rightarrow (^2D^o) 6s \ ^3D_1^o$	14, 15, 25, 26(G, P)
*A 6127.49 [39]	6127.	II	$(^2D^o) 6p \ ^3D_1 \rightarrow (^2D^o) 6s \ ^3D_2^o$	14, 15, 25, 26(G, P)
A 6585.21 [39]	6585.	II	$(^2D^o) 6p \ ^3D_1 \rightarrow (^2D^o) 6s \ ^3D_1^o$	15, 25(E), 26(G, P)
A 6904.77 [39]	6904.	II	$(^2D^o) 6p \ ^3D_2 \rightarrow (^2D^o) 6s \ ^1D_2^o$	25(E), 26(G, P)
A 7032.99 [39]	7032.	II	$(^2D^o) 6p \ ^3F_2 \rightarrow (^2D^o) 5d \ ^3D_2^o$	15, 25, 26(G, P)
A 8253.84 [39]	8250. ± 100	II	$(^2D^o) 6p \ ^3D_1 \rightarrow (^2D^o) 5d \ ^3P_0^o$	25, 26(G, P)
*A 8804.23 [39]	8800. ± 100	II	$(^2D^o) 6p \ ^3F_2 \rightarrow (^2D^o) 5d \ ^3F_3^o$	25, 26(G, P)

TABLE VIII		OXYGEN		
Calculated Wavelength in Å (Air)	Best Measured Wavelength in Å (Air)	Classification		References
* 2983.78	2983.86 ± 0.06	III	$(^2P^o) 3p \ ^1D_2 \rightarrow (^2P^o) 3s \ ^1P_1^o$	13(E), 20
3047.13	3047.15 ± 0.06	III	$(^2P^o) 3p \ ^3P_2 \rightarrow (^2P^o) 3s \ ^3P_2^o$	13(E), 20
3063.45	3063.46 ± 0.06	IV	$(^1S) 3p \ ^2P_{3/2}^o \rightarrow (^1S) 3s \ ^2S_{1/2}$	20
3381.33 Or 3381.28	3381.34 ± 0.06	IV	$\left\{ \begin{array}{l} (^3P^o) 3p \ ^4D_{3/2} \rightarrow (^3P^o) 3s \ ^4P_{1/2}^o \\ \text{Or} \\ (^3P^o) 3p \ ^4D_{5/2} \rightarrow (^3P^o) 3s \ ^4P_{3/2}^o \end{array} \right\}$	20
3385.54	3385.54 ± 0.06	IV	$(^3P^o) 3p \ ^4D_{7/2} \rightarrow (^3P^o) 3s \ ^4P_{5/2}^o$	20
3749.49	3749.49 ± 0.04	II	$(^3P) 3p \ ^4S_{3/2}^o \rightarrow (^3P) 3s \ ^4P_{5/2}$	12, 13, 20
3754.67	3754.68 ± 0.04	III	$(^2P^o) 3p \ ^3D_2 \rightarrow (^2P^o) 3s \ ^3P_1^o$	12, 13, 20
3759.88	3759.89 ± 0.05	III	$(^2P^o) 3p \ ^3D_3 \rightarrow (^2P^o) 3s \ ^3P_2^o$	12, 13, 20
* 4347.38	4347.38 ± 0.04	II	$(^1D) 3p \ ^2D_{3/2}^o \rightarrow (^1D) 3s \ ^2D_{3/2}$	12, 13
* 4351.28	4351.26 ± 0.04	II	$(^1D) 3p \ ^2D_{5/2}^o \rightarrow (^1D) 3s \ ^2D_{5/2}$	12, 13
* 4414.88	4414.93 ± 0.04	II	$(^3P) 3p \ ^2D_{5/2}^o \rightarrow (^3P) 3s \ ^2P_{3/2}$	12, 13
* 4416.97	4416.97 ± 0.04	II	$(^3P) 3p \ ^2D_{3/2}^o \rightarrow (^3P) 3s \ ^2P_{1/2}$	12, 13
. . . .	4605.52 ± 0.09	. . . .	. . . .	12
4649.14	4649.08 ± 0.1	II	$(^3P) 3p \ ^4D_{7/2}^o \rightarrow (^3P) 3s \ ^4P_{5/2}$	13
* 5592.37	5592.37 ± 0.06	III	$(^2P^o) 3p \ ^1P_1 \rightarrow (^2P^o) 3s \ ^1P_1^o$	12(E), 13, 31(E)
6721.36	6721.38 ± 0.04	II	$(^3P) 3p \ ^2S_{1/2}^o \rightarrow (^3P) 3s \ ^2P_{3/2}$	12(E)

TABLE IX		NITROGEN	
Calculated Wavelength in Å (Air)	Best Measured Wavelength in Å (Air)	Classification	References
3367.34	3367.32 ± 0.06	III $(^3P^o) 3p^4P_{5/2} \rightarrow (^3P^o) 3s^4P_{5/2}^o$	20
3478.67	3478.70 ± 0.06	IV $(^2S) 3p^3P_2^o \rightarrow (^2S) 3s^3S_1$	12, 20
3482.96	3483.02 ± 0.06	IV $(^2S) 3p^3P_1^o \rightarrow (^2S) 3s^3S_1$	20
4097.32	4097.29 ± 0.06	III $(^1S) 3p^2P_{3/2}^o \rightarrow (^1S) 3s^2S_{1/2}$	12
4103.38	4103.26 ± 0.07	III $(^1S) 3p^2P_{1/2}^o \rightarrow (^1S) 3s^2S_{1/2}$	12
4510.88	4510.45 ± 0.23	III $(^3P^o) 3p^4D_{5/2} \rightarrow (^3P^o) 3s^4P_{3/2}^o$	12
4514.87	4514.41 ± 0.23	III $(^3P^o) 3p^4D_{7/2} \rightarrow (^3P^o) 3s^4P_{5/2}^o$	12
4630.55	4630.31 ± 0.08	II $(^2P^o) 3p^3P_2 \rightarrow (^2P^o) 3s^3P_2^o$	12
5666.63	5666.62 ± 0.03	II $(^2P^o) 3p^3D_2 \rightarrow (^2P^o) 3s^3P_1^o$	27
5676.01	5676.03 ± 0.03	II $(^2P^o) 3p^3D_1 \rightarrow (^2P^o) 3s^3P_0^o$	27
* 5679.56	5679.53 ± 0.03	II $(^2P^o) 3p^3D_3 \rightarrow (^2P^o) 3s^3P_2^o$	13, 27, 31

TABLE X		MERCURY	
Calculated Wavelength in Å (Air)	Best Measured Wavelength in Å (Air)	Classification	References
4797.01	4797. ± 0.1	III $\left\{ \begin{array}{l} 5d^8 6s^2 (J=4) \rightarrow 5d^9 6p_{1/2} (J=3) \\ 126,468.3 \text{ cm}^{-1} \quad 105,627.8 \text{ cm}^{-1} \end{array} \right.$	8(G, P), 57
A 5677.3	5678. ± 1	II $5f^2F_{7/2}^o \rightarrow 6d^2D_{5/2}$	1(G, P), 3, 7, 8(G, P), 29
A 6149.9	6150. ± 1	II $7p^2P_{3/2}^o \rightarrow 7s^2S_{1/2}$	1(G, P), 3(G), 7, 8(G), 28, 29
A 7346.6	7346.	II $7d^2D_{5/2} \rightarrow 7p^2P_{3/2}^o$	1, 7
A 8549.8	8547.	II $5g^2G_{7/2} \rightarrow \text{"C"}^2F_{5/2}^o$	7
A 8622.	8628.	II $8p^2P_{3/2}^o \rightarrow \text{"4"}^2D_{5/2}^o$	7
A . . .	8677.	II?	7
A 9396.8	9396.	II $10s^2S_{1/2} \rightarrow 8p^2P_{3/2}^o$	7
A 10583.	10586.	II $8s^2S_{1/2} \rightarrow 7p^2P_{3/2}^o$	1, 7
A 11179.	11181.	II $7g^2G_{7/2} \rightarrow 6f^2F_{5/2}^o$	7
A . . .	12545.	II?	7
A . . .	12981.	II?	7
A . . .	13655.	II?	7
A 15555.	15550.	II $7p^2P_{3/2}^o \rightarrow 6d^2D_{5/2}$	7

TABLE XI		MISCELLANEOUS		
Calculated Wavelength in Å (Air)	Best Measured Wavelengths in Å (Air)	Classification	Discharge	References
. . .	3760.00 ± 0.04	. . .	Xe	13
4088.89	4088.90 ± 0.1	Si IV $4p^2 P_{3/2}^o \rightarrow 4s^2 S_{1/2}$	Ar	13
. . .	4645.3 ± 0.5	. . .	Ar	13
4647.45	4647.40 ± 0.04	C III $3p^3 P_2^o \rightarrow 3s^3 S_1$	CO <sub>2</sub> , Air, Kr, Xe	12, 13
4650.16	4650.11 ± 0.08	C III $3p^3 P_1^o \rightarrow 3s^3 S_1$	CO <sub>2</sub> , O <sub>2</sub>	12
. . .	4650.40 ± 0.1	. . .	Xe	13
. . .	6577.45 ± 0.12	. . .	He, Ne	13
. . .	12222.	Ar ?	Hg-Ar	28, 29
. . .	12246.	Ar ?	Hg-Ar	28, 29
. . .	12760.	Ar ?	Hg-Ar	28, 29

TABLE XII	SUMMARY												Totals
	Element												
	C	N	O	Ne	Si	Cl	Ar	Kr	I	Xe	Hg	?	
Ion Laser Lines Reported	2	11	16	16	1	9	39	40	12	63	14	7	230
Laser Lines Spectroscopically Confirmed	2	11	15	14	1	9	38	39	12	56	10	—	207
Laser Lines Classified	2	11	15	13	1	9	34	36	12	43	10	—	186
Core change only	0	0	0	0	0	0	7	2	2	4	0	—	15
Spin change only	0	0	0	1	0	0	2	10	1	3	1	—	18
Core and spin change	0	0	0	0	0	0	0	1	0	1	0	—	2

TABLE XII

## SUMMARY (CONTINUED)

	Element												Totals
	C	N	O	Ne	Si	Cl	Ar	Kr	I	Xe	Hg	?	
Laser Lines with J, L, S Known	2	11	15	12	1	9	34	36	12	33	9	—	174
No core or spin change	2	11	15	11	1	9	25	23	9	28	8	—	142
Also obeying $\Delta J = \Delta L$	1	9	15	7	1	8	20	15	4	19	8	—	107
Core change only	0	0	0	0	0	0	7	2	2	1	0	—	12
Also obeying $\Delta J = \Delta L$	0	0	0	0	0	0	7	0	1	1	0	—	9
Spin change only	0	0	0	1	0	0	2	10	1	3	1	—	18
Also obeying $\Delta J = \Delta L$	0	0	0	1	0	0	2	6	1	1	1	—	12
Core and spin change	0	0	0	0	0	0	0	1	0	1	0	—	2
Also obeying $\Delta J = \Delta L$	0	0	0	0	0	0	0	0	0	0	0	—	0

## CONCLUSIONS

Laser oscillation in gaseous ions has opened a new class of materials and excitation techniques for study. The results obtained in one year include pulsed and continuous operation at 230 wavelengths in the ultraviolet, visible, and infrared portions of the spectrum and higher power and gain than previously available in this region. The next year will, no doubt, see the development of practical ion laser sources to exploit these newly available characteristics in research and application.

*Note added in proof:* As we might have guessed, the field covered by this paper is moving faster than the pen or the presses. Laser oscillation has been obtained on several lines of ionized zinc, cadmium, sulfur, and phosphorus by Fowles, Jensen, and Silvast at University of Utah.

## ACKNOWLEDGMENT

A detailed list of acknowledgments would be almost as long as the list of references. We would like to thank the many people who have shared their most recent work with us. We also wish to acknowledge the many pleasant and productive discussions we have had with W. E. Bell, H. G. Cooper, L. Dana, E. I. Gordon, E. F. Labuda, R. A. McFarlane, and D. C. Sinclair. We would like to express our particular thanks to C. J. Humphreys, who so kindly supplied us with his unpublished listing of krypton and xenon lines.

## REFERENCES

- [1] Bell, W. E., Visible laser transitions in  $Hg^+$ , *Appl. Phys. Letters*, vol 4, Jan 15, 1964, pp 34-35.
- [2] Bridges, W. B., Laser oscillation in singly ionized argon in the visible spectrum, *Appl. Phys. Letters*, vol 4, Apr 1, 1964, pp 128-130.
- [3] Convert, G., M. Armand, and P. Martinot-Lagarde, Effet laser dans des mélanges mercure-gaz rares, *Compt. Rend. Acad. Sci. Paris*, vol 258, Mar 23, 1964, pp 3259-3260.
- [4] —, Transitions laser visibles dans l'argon ionisé, *Compt. Rend. Acad. Sci. Paris*, vol 258, May 4, 1964, pp 4467-4469.
- [5] Bennett, W. R., Jr., J. W. Knutson, Jr., G. N. Mercer, and J. L. Detch, Super-radiance, excitation mechanisms, and quasi-cw oscillation in the visible  $Ar^+$  laser, *Appl. Phys. Letters*, vol 4, May 15, 1964, pp 180-182.
- [6] Bridges, W. B., Laser action in singly ionized krypton and xenon, *Proc. IEEE (Correspondence)*, vol 52, Jul 1964, pp 843-844.
- [7] Bloom, A. L., W. E. Bell, and F. O. Lopez, Laser spectroscopy of a pulsed mercury-helium discharge, *Phys. Rev.*, vol 135, Aug 3, 1964, pp A578-A579.
- [8] Gerritsen, H. J., and P. V. Goedertier, Blue gas laser using  $Hg^{2+}$ , *J. Appl. Phys.*, vol 35, Oct 1964, pp 3060-3061.
- [9] Bell, W. E., and A. L. Bloom, private communication.
- [10] Gordon, E. I., E. F. Labuda, and W. B. Bridges, Continuous visible laser action in singly ionized argon, krypton, and xenon, *Appl. Phys. Letters*, vol 4, May 15, 1964, pp 178-180.
- [11] Gordon, E. I., and E. F. Labuda, Gas pumping in continuously operated ion lasers, *Bell Sys. Tech. J.*, vol 43, Jul 1964, pp 1827-1829.
- [12] McFarlane, R. A., Laser oscillation on visible and ultraviolet transitions of singly and multiply ionized oxygen, carbon, and nitrogen, *Appl. Phys. Letters*, vol 5, Sep 1, 1964, pp 91-93.
- [13] Bridges, W. B., and A. N. Chester, Visible and uv laser oscillation at 118 wavelengths in ionized neon, argon, krypton, xenon, oxygen and other gases, *Appl. Optics*, vol 4, May 1965, pp 573-580.
- [14] Fowles, G. R., and R. C. Jensen, Visible laser transitions in the spectrum of singly ionized iodine, *Proc. IEEE (Correspondence)*, vol 52, Jul 1964, pp 851-852.
- [15] —, Visible laser transitions in ionized iodine, *Appl. Optics*, vol 3, Oct 1964, pp 1191-1192.

- [16] McFarlane, R. A., Optical maser oscillation on iso-electronic transitions in Ar III and Cl II, *Appl. Optics*, vol 3, Oct 1964, p 1196.
- [17] Laures, P., L. Dana, and C. Frapard, Nouvelles transitions laser dans le domaine 0, 43-0, 52  $\mu$  obtenues à partir du spectre du krypton ionisé, *Compt. Rend. Acad. Sci. Paris*, vol 258, Jun 29, 1964, pp 6363-6365.
- [18] —, Nouvelles raies laser visibles dans le xenon ionisé, *Compt. Rend. Acad. Sci. Paris*, vol 259, Jul 27, 1964, pp 745-747.
- [19] Dana, L., and P. Laures, Stimulated emission in krypton and xenon ions by collisions with metastable atoms, *Proc. IEEE (Correspondence)*, vol 53, Jan 1965, pp 78-79.
- [20] Cheo, P. K., and H. G. Cooper, Ultraviolet ion laser transitions between 2300 Å and 4000 Å, *J. Appl. Phys.*, to be published; also *Bull. Am. Phys. Soc.*, vol 9, no 6, 1964, p 626.
- [21] Sinclair, D. C., Near-infrared oscillation in pulsed noble gas ion lasers, *J. Opt. Soc. Amer.*, vol 55, May 1965, pp 571-572.
- [22] Dana, L., P. Laures, and R. Rocherolles, Raies laser ultraviolettes dans le neon, l'argon et le xenon, *Compt. Rend. Acad. Sci. Paris*, vol 260, Jan 11, 1965, pp 481-484.
- [23] Horrigan, F. A., S. H. Koozekanani, and R. A. Paananen, Infrared laser action and lifetimes in Argon II, *Appl. Phys. Letters*, vol 6, Feb 1, 1965, pp 41-43.
- [24] Birnbaum, M., and T. L. Stocker, private communication.
- [25] Jensen, R. C., and G. R. Fowles, New laser transitions in iodine-inert gas mixtures, *Proc. IEEE (Correspondence)*, vol 52, Nov 1964, p 1350.
- [26] Fowles, G. R., private communication.
- [27] McFarlane, R. A., private communication.
- [28] Heard, H. G., G. Makhov, and J. Peterson, Laser action in mercury rare gas mixtures, *Proc. IEEE (Correspondence)*, vol 52, Apr 1964, p 414.
- [29] Heard, H. G., and J. Peterson, Mercury-rare gas visible-UV laser, *Proc. IEEE (Correspondence)*, vol 52, Sep 1964, pp 1049-1050.
- [30] —, Orange through blue-green transitions in a pulsed-cw xenon gas laser, *Proc. IEEE (Correspondence)*, vol 52, Sep 1964, p 1050.
- [31] —, Visible laser transitions in ionized oxygen, nitrogen and carbon monoxide, *Proc. IEEE (Correspondence)*, vol 52, Oct 1964, p 1258.
- [32] Heard, H. G., private communication.
- [33] Bennett, W. R., Jr., P. J. Kindlmann, G. N. Mercer, and J. Sunderland, Relaxation rates of the Ar<sup>+</sup> laser levels, *Appl. Phys. Letters*, vol 5, Oct 15, 1964, pp 158-160.
- [34] Gordon, E. I., E. F. Labuda, private communication.
- [35] Gordon, E. I., E. F. Labuda, R. C. Miller, and C. E. Webb, Excitation mechanisms of the argon ion laser, to be published.
- [36] Moore, C. E., Atomic energy levels, *Nat. Bur. Stand. (USA)*, *Circ. 467*, vol I, 1949, vol II, 1952, vol III, 1958.
- [37] Coleman, C. D., W. R. Bozman, W. F. Meggers, Table of wavenumbers, *Nat. Bur. Stand. (USA)*, *Monograph 3*, 1960.
- [38] Minnhagen, L., The spectrum of singly ionized argon, Ar II, *Ark. Fys.*, vol 25, 1963, pp 203-284.
- [39] Martin, W. C., and C. H. Corliss, The spectrum of singly ionized atomic iodine (I II), *J. Res. Nat. Bur. Stand. (USA)*, vol 64A, Dec 1960, pp 443-479.
- [40] Humphreys, C. J., private communication. Dr. Humphreys, now at the Naval Ordnance Lab., Corona, Calif., has kindly supplied us with a copy of his unpublished listing of krypton and xenon lines observed at the Bureau of Standards, 1930-1940.
- [41] deBruin, T. L., Über das zweite funkenspectrum des neons, Ne III, *Z. Phys.*, vol 77, Aug 1932, pp 505-514.
- [42] Rosenthal, A. H., Die wellenlängen des blauen argonspectrums (mit beiträgen zur termanalyse), *Ann. Phys.*, vol 4, ser 5, Jan 1930, pp 49-81.
- [43] Kayser, H., and H. Konen, *Handbuch der Spectroscopie*, vol 8, pt 1 Leipzig, Germany: S. Hirzel Verlag, 1932, p 97.
- [44] *Ibid.*, vol 6, p 819.
- [45] deBruin, T. L., and C. J. Bakker, Struktur und zeemaneffekt des neon funkenspectrums, Ne II, *Z. Phys.*, vol 69, Apr 1931, pp 19-35.
- [46] Bridges, W. B., and A. N. Chester, unpublished data.
- [47] Minnhagen, L., and L. Stigmark, The excitation of ionic spectra by 100 kW high frequency pulses, *Ark. Fys.*, vol 13, Feb 1958, pp 27-36.
- [48] Harrison, G. R., *MIT Wavelength Tables*. New York: Wiley, 1939.
- [49] Paananen, R. A., private communication.
- [50] Sinclair, D. C., private communication.
- [51] deBruin, T. L., C. J. Humphreys, and W. F. Meggers, The second spectrum of krypton, *J. Res. Nat. Bur. Stand. (U.S.)*, vol 11, Sep 1933, pp 409-440.
- [52] Humphreys, C. J., Third spectrum of xenon, *J. Res. Nat. Bur. Stand. (U.S.)*, vol 16, Jun 1936, pp. 639-648.
- [53] —, Second spectrum of xenon, *J. Res. Nat. Bur. Stand. (U.S.)*, vol 22, Jan 1939, pp. 19-53.
- [54] —, W. F. Meggers, and T. L. deBruin, Zeeman effect in the second and third spectra of xenon, *J. Res. Nat. Bur. Stand. (U.S.)*, vol 23, Dec 1939, pp 683-699. Note that this paper corrects classification errors in [52] and [53].
- [55] Dana, L., private communication.
- [56] Cooper, H. G., private communication.
- [57] Gerritsen, H. J., private communication.
- [58] Goldsmith, S., and A. S. Kaufman, The spectra of Ne IV, Ne V, and Ne VI: a further analysis, *Proc. Phys. Soc. (GB)*, vol 81, Mar 1963, pp 544-552.
- [59] Condon, E. V., and G. H. Shortley, *Theory of Atomic Spectra*. New York: Cambridge, 1953, pp 240-243.
- [60] Faust, W. L., R. A. McFarlane, C. K. N. Patel, and C. G. B. Garrett, Noble gas optical maser lines at wavelengths between 2 and 35 $\mu$ , *Phys. Rev.*, vol 133, Mar 16, 1964, pp A1476-A1486.
- [61] Bates, D. R., and Agnete Damgaard, The calculation of absolute strengths of spectral lines, *Phil. Trans. (GB)*, vol A242, 1949, pp 101-120.
- [62] Statz, H., private communication.
- [63] Griem, H. R., Coulomb approximation oscillator strengths of spectral lines from light and medium elements, Naval Research Lab. Rept. 6085, Jun 16, 1964; repeated in *Plasma Spectroscopy*, New York: McGraw-Hill, 1964, pp 363-440.